Biochimica et Biophysica Acta 1840 (2014) 2776–2782

Contents lists available at ScienceDirect

Biochimica et Biophysica Acta

journal homepage: www.elsevier.com/locate/bbagen

Metal-mediated oxidative DNA damage induced by methylene blue

Yusuke Hiraku [a,*], Hiroyuki Goto [a], Masaki Kohno [a], Shosuke Kawanishi [b], Mariko Murata [a]

[a] Department of Environmental and Molecular Medicine, Mie University Graduate School of Medicine, Tsu, Mie 514-8507, Japan
[b] Faculty of Pharmaceutical Sciences, Suzuka University of Medical Science, Suzuka, Mie 513-8670, Japan

ARTICLE INFO

Article history:
Received 3 March 2014
Received in revised form 24 April 2014
Accepted 25 April 2014
Available online 2 May 2014

Keywords:
Methylene blue
DNA damage
Metal ion
Reactive oxygen species
NADH
Carcinogenesis

ABSTRACT

Background: Methylene blue (MB) is used for various clinical purposes, including chromoendoscopy and methemoglobinemia treatment. However, MB induces tumors of pancreatic islets and small intestine in experimental animals. This finding raises a possibility that MB induces carcinogenicity in these organs via light-independent mechanisms, although MB is known to cause light-dependent DNA damage.
Methods: We investigated the mechanism of MB-induced DNA damage using ^{32}P-5′-end-labeled DNA fragments of human tumor-relevant genes. We investigated the redox reaction of MB by UV–visible spectrometry.
Results: MB induced DNA damage at the 5′-ACG-3′ sequence, a hot spot of the *p53* gene, in the presence of NADH and Cu(II). DNA damage was inhibited by catalase and bathocuproine, a Cu(I)-specific chelator. MB induced DNA damage at every nucleotide in the presence of NADH and Fe(III)-ethylenediaminetetraacetic acid, which was inhibited by •OH scavengers and catalase. MB significantly increased the formation of 8-oxo-7,8-dihydro-2′-deoxyguanosine, an oxidative DNA lesion, in the presence of NADH and metal ions. UV–visible spectrometry revealed that the absorbance of oxidized form of MB at 668 nm was decreased by NADH, and the addition of metal ions attenuated the spectral change.
Conclusions: MB undergoes NADH-dependent reduction followed by metal ion-mediated reoxidation. Reduced metal ions [Cu(I) and Fe(II)] interact with H_2O_2, generated during the redox reaction, to produce Cu(I)OOH and •OH that cause DNA damage, respectively. These findings suggest that metal-mediated DNA damage contributes to MB-mediated carcinogenesis.
General significance: This study would provide an insight into the mechanism of MB-induced carcinogenesis and its safety assurance for clinical use.

1. Introduction

Methylene blue (MB) has been clinically used to reverse methemoglobinemia caused by genetic deficiencies and metabolic poisoning [1]. MB is widely used as a very efficient dye for chromoendoscopy, which optimizes the evaluation of premalignant gastric lesions [2]. MB has been introduced in sentinel lymph node mapping of gastrointestinal and breast cancer [3,4]. Recent animal experiment revealed that MB photodynamic therapy induced a significant decrease in tumor volume and weight in a mouse model [5]. Moreover, clinical applications of MB for other purposes have been reported [6,7].

It is known that MB exposed to ultraviolet light (UV) or visible light causes guanine-specific DNA damage via the generation of singlet oxygen ($^1O_2$) [8–10]. Actually, the amount of oxidative DNA lesions was increased in Barrett's mucosa after chromoendoscopy, due to the presence of MB and endoscopic white light [11]. Recently, National Toxicology Program (NTP) has reported that there was some evidence for the carcinogenic activity of MB in experimental animals. Oral administration of MB increased the incidences of pancreatic islet cell adenoma or carcinoma in male rats and carcinoma in the small intestine in male mice [12,13]. This finding raises a possibility that light-independent DNA damage participates in MB-induced carcinogenesis in these abdominal organs. In addition, MB was mutagenic in some strains of *Salmonella typhimurium* and *Escherichia coli* with and without liver S9 [12]. It has been reported that MB is reduced by endogenous reductants, including NAD(P)H, and then accumulates in cells, although a precise mechanism remains to be clarified [14]. We have demonstrated that a wide variety of carcinogenic chemicals are reduced by NADH and induce DNA damage in the presence of metal ions, which catalyze the generation of reactive oxygen species (ROS) [15,16]. These findings led us to an idea that MB may induce metal-dependent oxidative DNA damage, which contributes to carcinogenesis.

Abbreviations: MB, methylene blue; UV, ultraviolet light; $^1O_2$, singlet oxygen; NTP, National Toxicology Program; ROS, reactive oxygen species; 8-oxodG, 8-oxo-7,8-dihydro-2′-deoxyguanosine; HPLC–ECD, an electrochemical detector coupled to HPLC; DTPA, diethylenetriamine-*N*,*N*,*N*′,*N*″,*N*″-pentaacetic acid; SOD, superoxide dismutase; Fpg, *E. coli* formamidopyrimidine-DNA glycosylase; EDTA, ethylenediaminetetraacetic acid; ANOVA, analysis of variance; $O_2^{\bullet -}$, superoxide; H_2O_2, hydrogen peroxide; •OH, hydroxyl free radical

* Corresponding author. Tel./fax: +81 59 231 5011.
E-mail address: y-hiraku@doc.medic.mie-u.ac.jp (Y. Hiraku).

http://dx.doi.org/10.1016/j.bbagen.2014.04.020
0304-4165/

In this study, we examined the mechanism of MB-induced DNA damage using ^{32}P-5′-end-labeled DNA fragments obtained from the human c-Ha-*ras* protooncogene and *p53* tumor suppressor gene in the presence of NADH and endogenous metal ions. We also quantified the formation of an oxidative DNA lesion, 8-oxo-7,8-dihydro-2′-deoxyguanosine (8-oxodG), using an electrochemical detector coupled to HPLC (HPLC–ECD). 8-OxodG is a mutagenic DNA lesion, which causes DNA misreplication and resulting G → T transversions [17,18]. We also performed UV–visible spectrometry to investigate NADH- and metal-mediated redox reaction of MB and ROS generation.

2. Materials and methods

2.1. Materials

[γ-^{32}P]-ATP (222 TBq/mmol) was from New England Nuclear (Boston, MA, USA). Restriction enzymes (*Ava*I, *Xba*I *Pst*I and *Hind*III) and T_4 polynucleotide kinase were purchased from New England Biolabs (Beverly, MA, USA). Restriction enzymes (*Eco*RI and *Apa*I) and calf intestine phosphatase were from Roche (Mannheim, Germany). MB and nuclease P_1 were from Wako Pure Chemical Industries Ltd. (Osaka, Japan). Diethylenetriamine-*N*,*N*,*N*′,*N*″,*N*″-pentaacetic acid (DTPA) and bathocuproinedisulfonic acid were from Dojin Chemicals Co. (Kumamoto, Japan). Calf thymus DNA, superoxide dismutase (CuZn-SOD, 3000 units/mg from bovine erythrocytes) and catalase (45,000 units/mg from bovine liver) were from Sigma Chemical Co. (St. Louis, MO, USA). *E. coli* formamidopyrimidine-DNA glycosylase (Fpg) was from Trevigen Co. (Gaithersburg, MD, USA). Deferoxamine was purchased from Novartis Pharma (Tokyo, Japan).

2.2. Preparation of ^{32}P-5′-end-labeled DNA fragments

DNA fragments were obtained from the human *p53* tumor suppressor gene [19]. The 5′-end-labeled 650-base pair fragment (*Hind*III* 13972–*Eco*RI* 14621, asterisk indicates ^{32}P-labeling) was obtained by dephosphorylation with calf intestine phosphatase and rephosphorylation with [γ-^{32}P]ATP and T_4 polynucleotide kinase as described previously [20]. This fragment was digested with *Apa*I to obtain a singly labeled 443-base pair (*Apa*I 14179–*Eco*RI* 14621) DNA fragment. DNA fragments were also prepared from plasmid pbcNI, which carries a 6.6-kb *Bam*HI chromosomal DNA segment containing the human c-Ha-*ras*-1 protooncogene [21,22]. A singly labeled 261-base pair fragment (*Ava*I* 1645–*Xba*I 1905) and a 337-base pair fragment (*Pst*I 2345–*Ava*I* 2681) were obtained as described previously [21,22]. Nucleotide numbering starts with the *Bam*HI site [23].

2.3. Detection of MB-induced damage to ^{32}P-labeled DNA fragments

The standard reaction mixtures in microtubes (1.5-ml Eppendorf) contained MB, 100 μM NADH, 20 μM $CuCl_2$ or Fe(III)-ethylenediaminetetraacetic acid (EDTA), ^{32}P-labeled DNA fragment and 10 μM/base calf thymus DNA in 10 mM sodium phosphate buffer (pH 7.8) containing 5 μM DTPA. The mixtures were covered with aluminum foil to avoid light exposure and incubated for 1 h at 37 °C. In a certain experiment, the mixture (without NADH and metal ion) was exposed to 10 J/cm^2 UVA (365 nm) as described previously [24]. After ethanol precipitation, the DNA fragments were heated in 1 M piperidine for 20 min at 90 °C or treated with 5 units of Fpg for 2 h at 37 °C. Fpg protein catalyzes the excision of 8-oxodG as well as Fapy residues [25]. Subsequently, DNA fragments were denatured by heating for 1 min at 90 °C followed by chilling on ice and electrophoresed on an 8% polyacrylamide/8 M urea gel. Then the autoradiogram was obtained by exposing an X-ray film to the gel. The preferred cleavage sites were determined by direct comparison of the positions of the oligonucleotides with those produced by the chemical reactions of the Maxam–Gilbert procedure [26] using a DNA-sequencing system (LKB 2010 Macrophor, Pharmacia LKB Biotechnology, Uppsala, Sweden). A laser densitometer (Personal Densitometer SI, Amarsham Biosciences, Uppsala, Sweden) was used for the measurement of the relative amounts of oligonucleotides from the treated DNA fragments.

2.4. Measurement of 8-oxodG formation induced by MB

The amount of 8-oxodG was measured by a modified method of Kasai et al. [27]. The reaction mixtures containing 100 μM/base calf thymus DNA, MB, 100 μM NADH and 20 μM $CuCl_2$ or Fe(III)EDTA in 4 mM sodium phosphate buffer (pH 7.8) containing 5 μM DTPA were incubated for 1 h at 37 °C. After ethanol precipitation, DNA was digested to the nucleosides with nuclease P_1 and calf intestine phosphatase, and analyzed with an HPLC–ECD as described previously [28]. Statistical analysis was performed by two-way analysis of variance (ANOVA) followed by Tukey's test using an IBM SPSS Statistics software version 20 for Macintosh. p values less than 0.05 were considered to be statistically significant.

2.5. UV–visible spectra of MB plus NADH and metal ions

UV–visible spectra were measured with a UV–visible spectrometer (UV-2500PC, Shimadzu, Kyoto, Japan). The reaction mixtures contained 10 μM MB, 100 μM NADH and 20 μM $CuCl_2$ or Fe(III)EDTA in 10 mM sodium phosphate buffer (pH 7.8) containing 5 μM DTPA. The spectra of the mixture were measured repeatedly at 37 °C every 5 min for 30 min, and the absorbance at 668 nm, the maximum absorption of oxidized form of MB, was traced.

2.6. Superoxide (O_2•$^-$) generation during the reaction of MB with NADH and metal ions

To examine MB-mediated O_2•$^-$ generation, a maximum absorption at 550 nm due to ferrocytochrome c formed by ferricytochrome c reduction was measured at 37 °C with a UV–visible spectrophotometer (UV-2500PC, Shimadzu). The reaction mixtures contained 10 μM MB, 100 μM NADH, no or 20 μM metal ions [$CuCl_2$ or Fe(III)EDTA] and 50 μM cytochrome c with or without 150 units/mL SOD in 10 mM sodium phosphate buffer (pH 7.8) containing 5 μM DTPA. The spectral tracing was repeated every 5 min for 30 min at 37 °C. The actual amount of O_2•$^-$ generation was calculated by subtracting the absorbance with SOD from that without SOD at 550 nm ($\varepsilon = 21.1 \times 10^3\ M^{-1}\ cm^{-1}$) [29].

3. Results

3.1. MB-induced damage to ^{32}P-labeled DNA fragments

Fig. 1 shows an autoradiogram of DNA fragments treated with MB in the presence of NADH and metal ions. Oligonucleotides were detected on the autoradiogram as a result of DNA cleavage. MB caused DNA damage in the presence of NADH and Cu(II) (Fig. 1A) or Fe(III)EDTA (Fig. 1B) in a dose-dependent manner. Cu(II)-mediated DNA damage was stronger than that mediated by Fe(III)EDTA. MB did not cause DNA damage in the absence of NADH or metal ions.

3.2. Effects of scavengers and metal chelators on MB-induced DNA damage

The effects of scavengers and metal chelators on MB-induced DNA damage are shown in Fig. 2. MB-induced DNA damage in the presence of NADH and Cu(II) was inhibited by catalase and bathocuproine, a Cu(I) chelator, suggesting that hydrogen peroxide (H_2O_2) and Cu(I) were involved (Fig. 2A). Typical hydroxyl free radical (•OH) scavengers (ethanol, mannitol, sodium formate and methional) did not inhibit the DNA damage (Fig. 2A). MB-induced DNA damage in the presence of

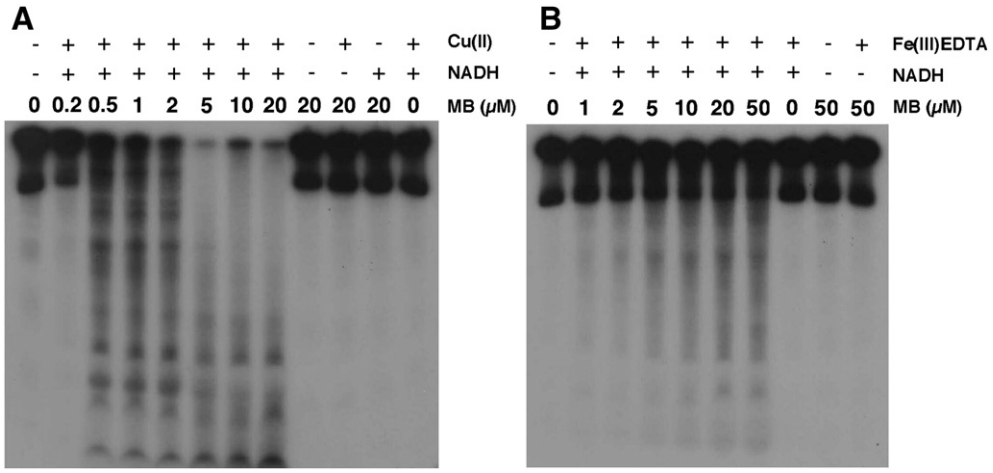

Fig. 1. Autoradiogram of ^{32}P-5′-end-labeled DNA fragments incubated with MB in the presence of NADH and metal ions. The reaction mixtures contained the ^{32}P-5′-end-labeled 443-base pair DNA fragments, 10 μM/base of sonicated calf thymus DNA, indicated concentration of MB, 100 μM NADH and 20 μM $CuCl_2$ (A) or Fe(III)EDTA (B) in 10 mM sodium phosphate buffer (pH 7.8) containing 5 μM DTPA, and were incubated for 1 h at 37 °C. Then, the DNA fragments were treated with 1 M piperidine for 20 min at 90 °C. DNA fragments were electrophoresed and the autoradiogram was obtained as described in the Materials and methods section.

NADH and Fe(III)EDTA was inhibited by catalase, •OH scavengers and deferoxamine, an iron chelator, suggesting that H_2O_2, •OH and iron were involved (Fig. 2B). SOD slightly reduced DNA damage in the presence of Cu(II) (Fig. 2A), but not in the presence of Fe(III)EDTA (Fig. 2B). DNA damage without piperidine treatment was weaker than that with the treatment, suggesting that MB plus metal ions induced not only strand breakage but also base modification (Fig. 2A and B).

3.3. Site specificity of MB-induced DNA damage

Figs. 3 and 4 show the site specificity of MB-induced DNA damage in the presence of NADH and Cu(II) (Figs. 3A, B and 4A) or Fe(III)EDTA (Fig. 4B). MB induced piperidine–labile lesions frequently at thymine and cytosine residues in the presence of NADH and Cu(II) (Figs. 3A and 4A), whereas Fpg treatment induced cleavage at guanine and cytosine residues (Fig. 3B). A double base lesion occurred at cytosine (piperidine–labile) and guanine (Fpg-sensitive) residues in the 5′-ACG-3′ sequence, which is complementary to the sequence of codon 273, a mutational hot spot of the *p53* gene (Fig. 3A and B). In the presence of NADH and Fe(III)EDTA, MB induced damage to every nucleotide (Fig. 4B). MB plus UVA caused DNA damage at every guanine residue (Fig. 3C) and showed a different site specificity from MB plus metal ions.

3.4. MB-induced 8-oxodG formation

By using an HPLC–ECD, we measured the content of 8-oxodG, an indicator of oxidative DNA damage, in calf thymus DNA treated with MB plus NADH and metal ions. MB increased 8-oxodG formation in a

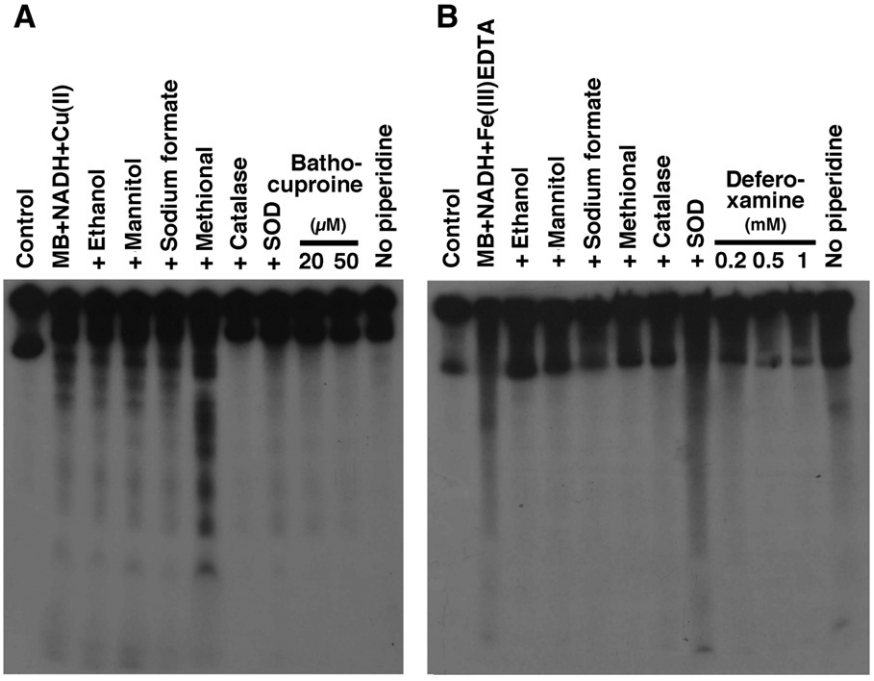

Fig. 2. Effects of scavengers and metal chelators on MB-induced DNA damage in the presence of NADH and metal ions. The reaction mixtures contained the ^{32}P-5′-end-labeled 337-base pair DNA fragments, 10 μM/base of sonicated calf thymus DNA, 2 μM (A) or 10 μM (B) MB, 100 μM NADH, 20 μM $CuCl_2$ (A) or Fe(III)EDTA (B) and scavenger [5% (v/v) ethanol, 0.1 M mannitol, 0.1 M sodium formate, 0.1 M methional, 150 units/mL catalase or 150 units/mL SOD] or metal chelator [bathocuproine (A) or deferoxamine (B)] in 10 mM sodium phosphate buffer (pH 7.8) containing 5 μM DTPA, and were incubated for 1 h at 37 °C. After the incubation, DNA fragments were treated with piperidine and then analyzed as described in Fig. 1. Control contained none of MB, metal ions or NADH.

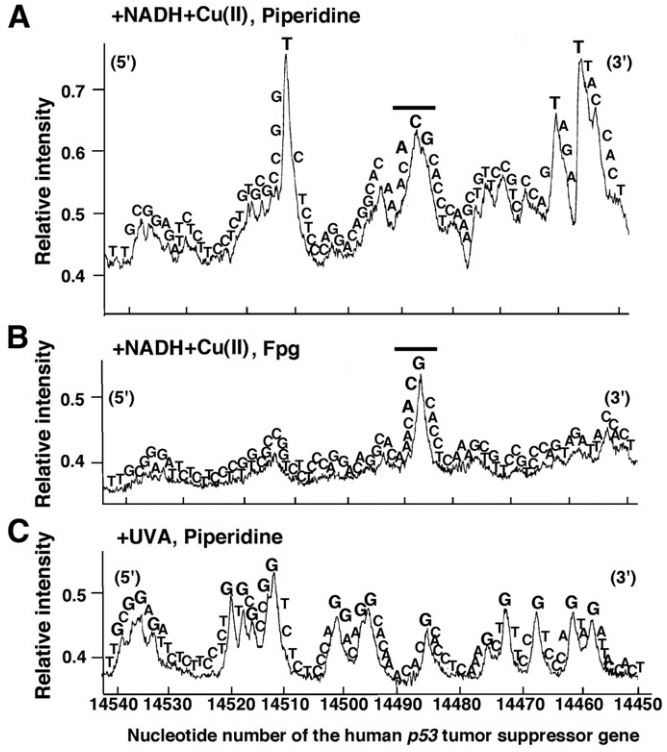

Fig. 3. Site specificity of Cu(II)- and UVA-mediated DNA damage induced by MB. (A, B) The reaction mixtures contained the ^{32}P-5′-end-labeled 443-base pair DNA fragments, 10 μM/base of sonicated calf thymus DNA, 0.5 μM MB, 100 μM NADH and 20 μM $CuCl_2$ in 10 mM sodium phosphate buffer (pH 7.8) containing 5 μM DTPA, and were incubated for 1 h at 37 °C. (C) The reaction mixture contained the ^{32}P-5′-end-labeled 443-base pair DNA fragments, 10 μM/base of sonicated calf thymus DNA and 0.5 μM MB in 10 mM sodium phosphate buffer (pH 7.8) containing 5 μM DTPA, and was exposed to 10 J/cm^2 UVA (365 nm). Then, DNA fragments were treated with 1 M piperidine for 20 min at 90 °C (A, C) or 5 units of Fpg for 2 h at 37 °C (B). DNA fragments were electrophoresed and the autoradiogram was obtained as described in the Materials and methods section. The relative intensity of DNA damage was measured by scanning the autoradiogram with a laser densitometer. Horizontal axis is the nucleotide number of the human *p53* tumor suppressor gene. Bar, the 5′-ACG-3′ sequence complementary to the sequence of codon 273, a mutational hot spot.

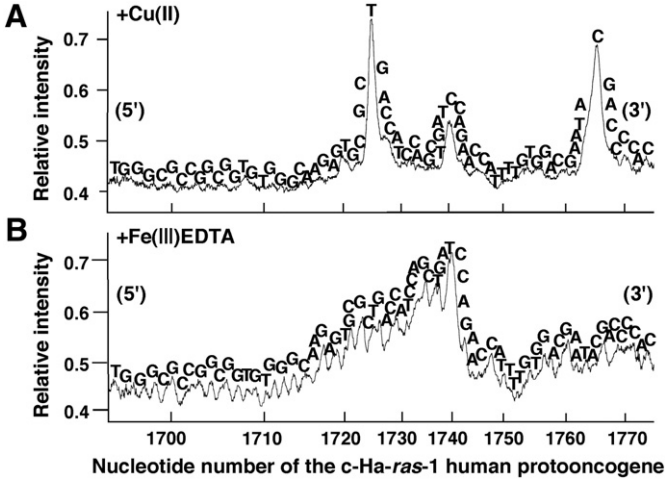

Fig. 4. Site specificity of metal-mediated DNA damage induced by MB. The reaction mixtures contained the ^{32}P-5′-end-labeled 261-base pair DNA fragments, 10 μM/base of sonicated calf thymus DNA, 2 μM (A) or 10 μM MB (B), 100 μM NADH and 20 μM $CuCl_2$ (A) or Fe(III)EDTA (B) in 10 mM sodium phosphate buffer (pH 7.8) containing 5 μM DTPA. After the incubation for 1 h at 37 °C, the DNA fragments were treated with piperidine and then analyzed by the method described in Fig. 3. Horizontal axis is the nucleotide number of the human c-Ha-*ras*-1 protooncogene.

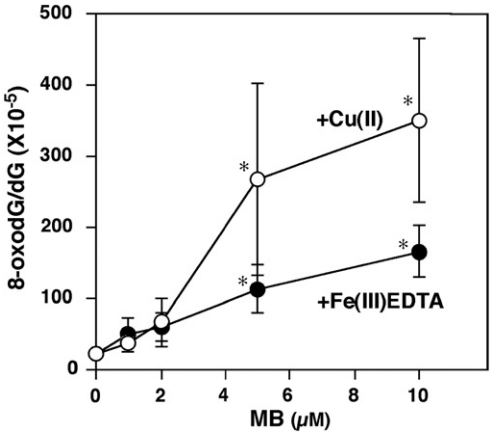

Fig. 5. Formation of 8-oxodG induced by MB in the presence of NADH and metal ions. The reaction mixtures contained 100 μM/base of calf thymus DNA, indicated concentration of MB, 100 μM NADH and 20 μM $CuCl_2$ or Fe(III)EDTA in 4 mM sodium phosphate buffer (pH 7.8) containing 5 μM DTPA, and were incubated for 1 h at 37 °C. The DNA fragments were enzymatically digested into nucleosides, and 8-oxodG formation was analyzed with an HPLC–ECD. *$p < 0.001$, compared with control (NADH plus metal ions without MB, two-way ANOVA followed by Tukey's test).

dose-dependent manner, and MB formed larger amount of this DNA lesion in the presence of Cu(II) than in the presence of Fe(III)EDTA at 5 and 10 μM (Fig. 5). Two-way ANOVA revealed that MB concentrations ($F = 38.906$, $p < 0.001$) and metal ions [Cu(II) or Fe(III)EDTA] ($F = 20.790$, $p < 0.001$) significantly influenced 8-oxodG formation, and that the interaction between these factors was also significant ($F = 8.150$, $p < 0.001$). Post hoc Tukey's test revealed that MB significantly increased 8-oxodG formation at 5 and 10 μM compared with the control ($p < 0.001$, Fig. 5).

3.5. Spectral change induced by MB plus NADH and effects of metal ions

We examined the change in UV–visible spectra of MB in the presence of NADH and metal ions. The absorbance at 668 nm, the maximal absorption of oxidized form of MB, was time-dependently decreased in the presence of NADH without metal ions (Fig. 6A). Addition of Cu(II) or Fe(III)EDTA attenuated the spectral change mediated by MB + NADH (Fig. 6A). The time course of the change in the absorbance at 668 nm (ΔAbsorbance) is shown in Fig. 6B. ΔAbsorbance mediated by MB + NADH was decreased by the addition of metal ions. Similar time courses were observed in the presence of Cu(II) and Fe(III)EDTA (Fig. 6B).

3.6. $O_2^{\bullet -}$ generation induced by MB plus NADH and metal ions

We examined MB-mediated $O_2^{\bullet -}$ generation by UV–visible spectrometry. In the presence of MB plus NADH without metal ions, slight $O_2^{\bullet -}$ generation was observed (Fig. 7), probably due to the reaction of O_2 with NAD• produced by NADH oxidation during MB reduction. The addition of Cu(II) or Fe(III)EDTA to MB plus NADH enhanced $O_2^{\bullet -}$ generation, which was increased in a time-dependent manner (Fig. 7).

4. Discussion

In this study, we firstly demonstrated that MB caused oxidative DNA damage in the presence of NADH and metal ions, Cu(II) and Fe(III)EDTA. MB required both NADH and metal ions for DNA damage, raising a possibility that MB is reduced by NADH and that metal ions mediate the generation of reactive species. Inhibitory effects of catalase and bathocuproine on Cu(II)-mediated DNA damage indicate that H_2O_2 and Cu(I) were involved in DNA damage via the formation of metal–oxygen complexes, such as Cu(I)–OOH. No or weak inhibitory effect of typical •OH scavengers on DNA damage was observed, suggesting that

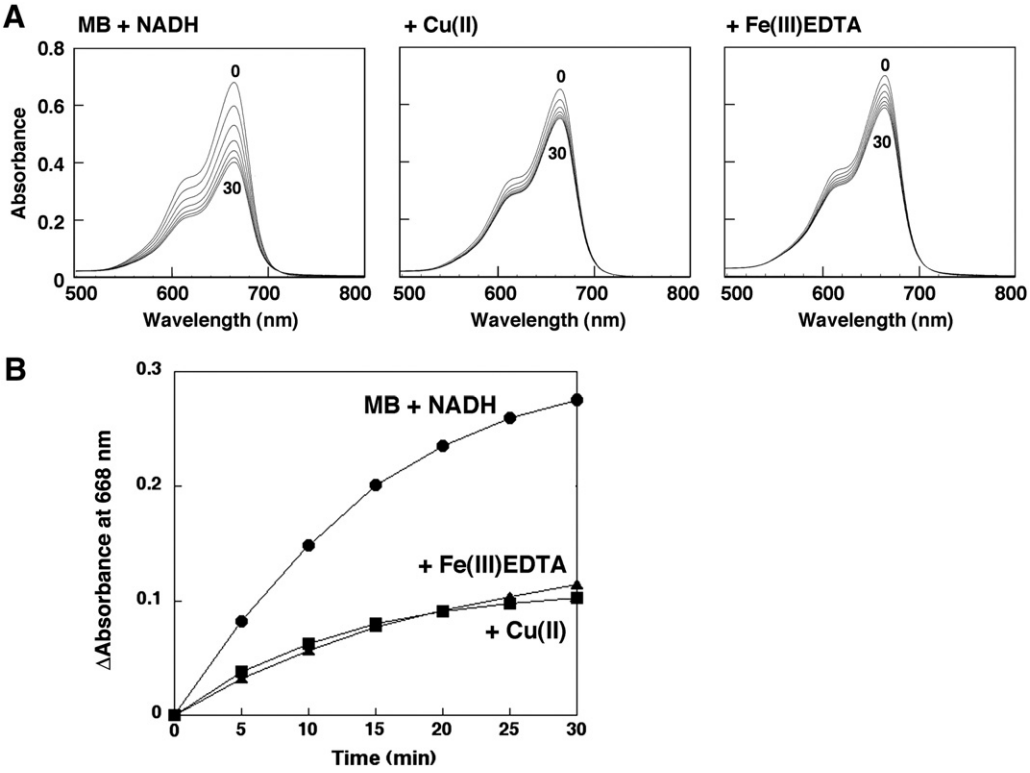

Fig. 6. Spectral change of MB in the presence of NADH and effects of metal ions. The reaction mixtures contained 10 μM MB, 100 μM NADH and no or 20 μM metal ions [$CuCl_2$ or Fe(III)EDTA] in 10 mM sodium phosphate buffer (pH 7.8) containing 5 μM DTPA. (A) Time-dependent spectral change of MB. The spectral tracing was repeated every 5 min for 30 min at 37 °C. (B) Time course of the decrease in the absorbance (ΔAbsorbance) at 668 nm, the maximum absorption wavelength of oxidized form of MB. ΔAbsorbance was calculated by subtraction of the absorbance at 668 nm at each time point from that at 0 min.

•OH does not play a key role. On the other hand, Fe(III)EDTA-mediated DNA damage was inhibited by catalase, •OH scavengers and deferoxamine, indicating that H_2O_2, •OH and iron were involved. SOD showed a slight inhibitory effect on Cu(II)-mediated DNA damage, but not on Fe(III)EDTA-mediated damage. Previous biochemical studies demonstrated that SOD reacts with not only $O_2{\bullet}^-$ but also H_2O_2 [30]. This finding raises a possibility that SOD also interacts with metal–peroxide complexes, including Cu(I)–OOH, resulting in partial inhibition of Cu(II)-mediated DNA damage, although the precise mechanism remains to be clarified.

These findings are supported by the site specificity of DNA damage. MB preferentially caused damage to the 5′-ACG-3′ sequence in the *p53* gene and thymine residues in the presence of NADH and Cu(II). The 5′-ACG-3′ sequence is complementary to codon 273, a known mutational hot spot of the *p53* gene [31]. We have demonstrated that

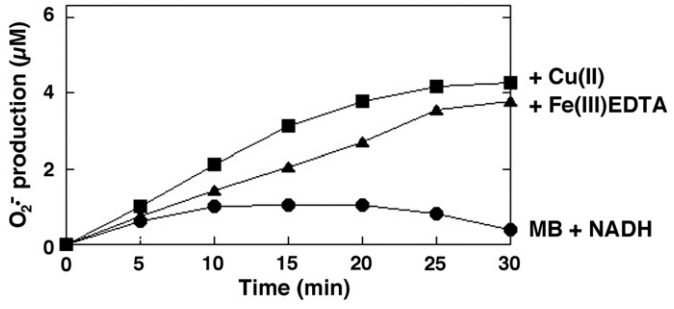

Fig. 7. $O_2{\bullet}^-$ generation during the reaction of MB with NADH and metal ions. The reaction mixtures contained 10 μM MB, 100 μM NADH, no or 20 μM metal ions [$CuCl_2$ or Fe(III)EDTA], 50 μM cytochrome c and no or 150 units/mL SOD in 10 mM sodium phosphate buffer (pH 7.8) containing 5 μM DTPA. The spectral tracing was repeated every 5 min for 30 min at 37 °C. The amount of $O_2{\bullet}^-$ generation was estimated by subtracting the amount of reduced cytochrome c in the presence of SOD from that in the absence of SOD.

various carcinogenic chemicals induce DNA damage in the presence of Cu(II), and showed a similar site specificity [16]. MB induced DNA damage in the presence of NADH and Fe(III)EDTA at every nucleotide, supporting the involvement of •OH [32,33]. UVA-irradiated MB induced guanine-specific DNA damage, and showed a different site specificity. Photoexcited MB is known to generate $^1O_2$, which forms guanine-specific DNA lesions, including 8-oxodG [10,34]. We have demonstrated that various UVA-irradiated photosensitizers generate $^1O_2$ to cause DNA damage specifically at guanine [35]. Recently, it has been reported that MB induced pancreatic islet cell carcinoma in rats and carcinoma in the small intestine in mice [12,13]. Our findings raise a possibility that MB interacts with endogenous metal ions to induce DNA damage independently of light exposure, which may participate in carcinogenesis in these organs.

UV–visible spectra showed that the absorbance of oxidized form of MB at 668 nm was decreased in the presence of NADH, and the addition of metal ions attenuated this spectral change. Reduced form of MB is known to be colorless [14]. This result suggests that MB is reduced by NADH, and undergoes metal-mediated reoxidation. This hypothesis is supported by a previous literature showing that MB stimulates the reduction of ferricyanide to ferrocyanide [14]. Although similar time courses of spectral change and $O_2{\bullet}^-$ generation were observed in the presence of Cu(II) and Fe(III)EDTA, Cu(II) mediated stronger damage to ^{32}P-labeled DNA fragments and 8-oxodG formation in calf thymus DNA treated with MB plus NADH than Fe(III)EDTA. These findings suggest that $O_2{\bullet}^-$ is dismutated to H_2O_2 and that Cu(II) plus H_2O_2 mediate stronger DNA damage than Fe(III)EDTA plus H_2O_2, as demonstrated in a previous study [36].

On the basis of our results, a proposed mechanism of MB-induced DNA damage is shown in Fig. 8. Oxidized form of MB is reduced by NADH and then reoxidized by Cu(II) and Fe(III), which are simultaneously reduced to Cu(I) and Fe(II), respectively. These metal ions are reoxidized to Cu(II) and Fe(III), and $O_2{\bullet}^-$ is concomitantly generated

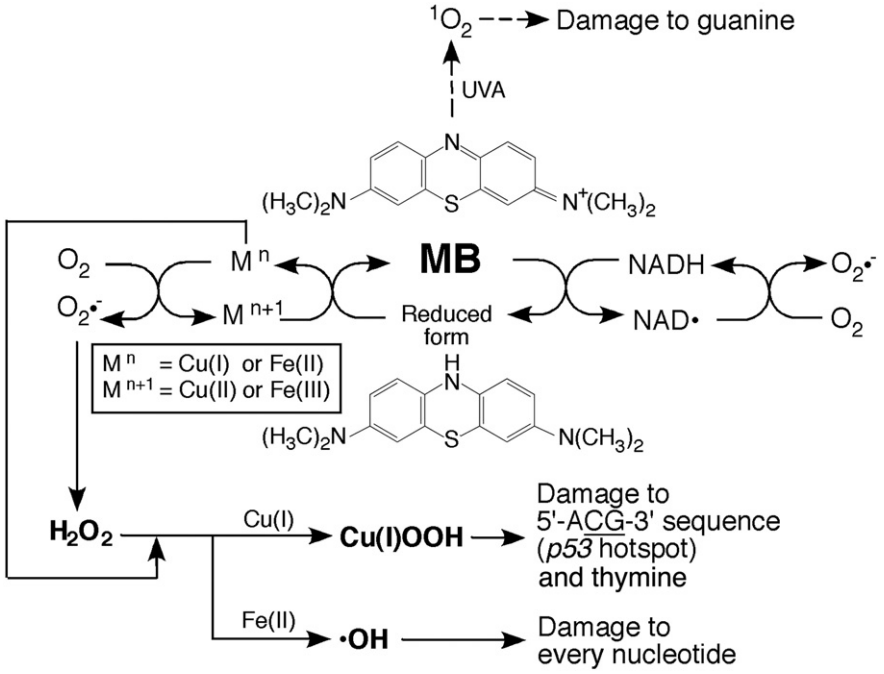

Fig. 8. Proposed mechanism of metal-mediated DNA damage induced by MB.

by reduction of molecular oxygen, followed by dismutation to H_2O_2. Eventually, H_2O_2 interacts with Cu(I) and Fe(II) to form Cu(I)OOH and •OH that are capable of causing DNA damage, respectively. We demonstrated that 8-oxodG formation in calf thymus DNA was significantly increased by MB plus NADH and metal ions. 8-OxodG formation causes DNA misreplication, which might lead to mutation, particularly G → T substitution [17,18].

Copper occurs in the mammalian cell nucleus, and may contribute to high order chromatin structures [37]. Copper ion binds to non-histone proteins, and causes much stronger ascorbate-mediated DNA damage than iron [38]. It has been reported that copper has an ability to catalyze ROS generation to cause DNA damage [15,16,39]. Iron is the most abundant transition metal ion in human body such as hemoglobin. High body stores of iron may increase the risk of cancer in humans [40]. Genetic alterations in the *p15* and *p16* tumor suppressor genes have been found in rats treated with Fe(III)-nitrilotriacetate [41]. The biological importance of NADH as a nuclear reductant has been reported [42]. NAD(P)H is contained in biological systems up to 100–200 μM [43]. Therefore, endogenous metal ions and NADH may play an important role in MB-induced DNA damage and carcinogenesis.

MB is known to accumulate in cells, and it is speculated that MB induces oxidative damage to cellular DNA as follows. Oxidized form of MB is impermeable to cell membrane. MB is reduced by endogenous reductants, including NADH, and to a lesser extent, glutathione and ascorbic acid [14]. Reduced form of MB is taken up by the cells and partially reoxidized and retained in the cell. Intracellular MB interacts with endogenous metal ions to generate ROS, resulting in DNA damage. Doses of MB used in chromoendoscopy reach millimolar levels [44], and thus intracellular concentration of MB is supposed to be extremely high. Therefore, experimental conditions in this study appear to be clinically relevant.

5. Conclusions

In this study, we demonstrated that MB induced oxidative DNA damage in the presence of NADH and metal ions via light-independent mechanisms. This finding raises a possibility that DNA damage mediated by endogenous metal ions contributes, at least in part, to MB-induced carcinogenesis. MB has been used for the treatment of methemoglobinemia, chromoendoscopy and a wide variety of other clinically purposes. This study would provide an insight into the mechanisms of MB-induced carcinogenesis and its safety assurance for clinical use.

Acknowledgements

This work was supported by Grants-in-Aid for Cancer Research from the Ministry of Health, Labour and Welfare of Japan (19-19) and the National Cancer Center Research and Development Fund (21-X-1-2).

References

[1] R.O. Wright, W.J. Lewander, A.D. Woolf, Methemoglobinemia: etiology, pharmacology, and clinical management, Ann. Emerg. Med. 34 (1999) 646–656.
[2] M. Areia, P. Amaro, M. Dinis-Ribeiro, M.A. Cipriano, C. Marinho, A. Costa-Pereira, C. Lopes, L. Moreira-Dias, J.M. Romaozinho, H. Gouveia, D. Freitas, M.C. Leitao, External validation of a classification for methylene blue magnification chromoendoscopy in premalignant gastric lesions, Gastrointest. Endosc. 67 (2008) 1011–1018.
[3] M. Soni, S. Saha, A. Korant, P. Fritz, B. Chakravarty, S. Sirop, A. Gayar, D. Iddings, D. Wiese, A prospective trial comparing 1% lymphazurin vs 1% methylene blue in sentinel lymph node mapping of gastrointestinal tumors, Ann. Surg. Oncol. 16 (2009) 2224–2230.
[4] C. Mathelin, S. Croce, D. Brasse, B. Gairard, M. Gharbi, N. Andriamisandratsoa, V. Bekaert, Z. Francis, J.L. Guyonnet, D. Huss, S. Salvador, R. Schaeffer, D. Grucker, C. Marin, J.P. Bellocq, Methylene blue dye, an accurate dye for sentinel lymph node identification in early breast cancer, Anticancer Res. 29 (2009) 4119–4125.
[5] M. Wagner, E.R. Suarez, T.R. Theodoro, C.D. Machado Filho, M.F. Gama, J.P. Tardivo, F. M. Paschoal, M.A. Pinhal, Methylene blue photodynamic therapy in malignant melanoma decreases expression of proliferating cell nuclear antigen and heparanases, Clin. Exp. Dermatol. 37 (2012) 527–533.
[6] H. Koelzow, J.A. Gedney, J. Baumann, N.J. Snook, M.C. Bellamy, The effect of methylene blue on the hemodynamic changes during ischemia reperfusion injury in orthotopic liver transplantation, Anesth. Analg. 94 (2002) 824–829.
[7] B. Coulibaly, A. Zoungrana, F.P. Mockenhaupt, R.H. Schirmer, C. Klose, U. Mansmann, P.E. Meissner, O. Muller, Strong gametocytocidal effect of methylene blue-based combination therapy against falciparum malaria: a randomised controlled trial, PLoS ONE 4 (2009) e5318.
[8] H.C. DeFedericis, H.B. Patrzyc, M.J. Rajecki, E.E. Budzinski, H. Iijima, J.B. Dawidzik, M. S. Evans, K.F. Greene, H.C. Box, Singlet oxygen-induced DNA damage, Radiat. Res. 165 (2006) 445–451.
[9] T. Friedmann, D.M. Brown, Base-specific reactions useful for DNA sequencing: methylene blue-sensitized photooxidation of guanine and osmium tetraoxide modification of thymine, Nucleic Acids Res. 5 (1978) 615–622.
[10] C. Maria Berra, C.S. de Oliveira, C.C. Machado Garcia, C.R. Reily Rocha, L. Koch Lerner, L.C. de Andrade Lima, M. da Silva Baptista, C.F. Martins Menck, Nucleotide excision repair activity on DNA damage induced by photoactivated methylene blue, Free Radic. Biol. Med. 61C (2013) 343–356.

[11] J.R. Olliver, C.P. Wild, P. Sahay, S. Dexter, L.J. Hardie, Chromoendoscopy with methylene blue and associated DNA damage in Barrett's oesophagus, Lancet 362 (2003) 373–374.
[12] NTP, NTP toxicology and carcinogenesis studies of methylene blue trihydrate (CAS no. 7220-79-3) in F344/N rats and B6C3F1 mice (gavage studies), Natl. Toxicol. Program Tech. Rep. Ser. (2008) 1–224.
[13] S.S. Auerbach, D.W. Bristol, J.C. Peckham, G.S. Travlos, C.D. Hebert, R.S. Chhabra, Toxicity and carcinogenicity studies of methylene blue trihydrate in F344N rats and B6C3F1 mice, Food Chem. Toxicol. 48 (2010) 169–177.
[14] J.M. May, Z.C. Qu, C.E. Cobb, Reduction and uptake of methylene blue by human erythrocytes, Am. J. Physiol. Cell Physiol. 286 (2004) C1390–C1398.
[15] S. Kawanishi, Y. Hiraku, M. Murata, S. Oikawa, The role of metals in site-specific DNA damage with reference to carcinogenesis, Free Radic. Biol. Med. 32 (2002) 822–832.
[16] S. Kawanishi, Y. Hiraku, Oxidative and nitrative DNA damage as biomarker for carcinogenesis with special reference to inflammation, Antioxid. Redox Signal. 8 (2006) 1047–1058.
[17] S. Shibutani, M. Takeshita, A.P. Grollman, Insertion of specific bases during DNA synthesis past the oxidation-damaged base 8-oxodG, Nature 349 (1991) 431–434.
[18] S.S. David, V.L. O'Shea, S. Kundu, Base-excision repair of oxidative DNA damage, Nature 447 (2007) 941–950.
[19] P. Chumakov, EMBL Data Library, (1990) Accession Number X54156.
[20] N. Yamashita, M. Murata, S. Inoue, Y. Hiraku, T. Yoshinaga, S. Kawanishi, Superoxide formation and DNA damage induced by a fragrant furanone in the presence of copper(II), Mutat. Res. 397 (1998) 191–201.
[21] S. Kawanishi, K. Yamamoto, Mechanism of site-specific DNA damage induced by methylhydrazines in the presence of copper(II) or manganese(III), Biochemistry 30 (1991) 3069–3075.
[22] K. Yamamoto, S. Kawanishi, Site-specific DNA damage induced by hydrazine in the presence of manganese and copper ions. The role of hydroxyl radical and hydrogen atom, J. Biol. Chem. 266 (1991) 1509–1515.
[23] D.J. Capon, E.Y. Chen, A.D. Levinson, P.H. Seeburg, D.V. Goeddel, Complete nucleotide sequences of the T24 human bladder carcinoma oncogene and its normal homologue, Nature 302 (1983) 33–37.
[24] K. Ito, Y. Hiraku, S. Kawanishi, Photosensitized DNA damage induced by NADH: site specificity and mechanism, Free Radic. Res. 41 (2007) 461–468.
[25] M.H. David-Cordonnier, J. Laval, P. O'Neill, Clustered DNA damage, influence on damage excision by XRS5 nuclear extracts and *Escherichia coli* Nth and Fpg proteins, J. Biol. Chem. 275 (2000) 11865–11873.
[26] A.M. Maxam, W. Gilbert, Sequencing end-labeled DNA with base-specific chemical cleavages, Methods Enzymol. 65 (1980) 499–560.
[27] H. Kasai, P.F. Crain, Y. Kuchino, S. Nishimura, A. Ootsuyama, H. Tanooka, Formation of 8-hydroxyguanine moiety in cellular DNA by agents producing oxygen radicals and evidence for its repair, Carcinogenesis 7 (1986) 1849–1851.
[28] K. Ito, S. Inoue, K. Yamamoto, S. Kawanishi, 8-Hydroxydeoxyguanosine formation at the 5′ site of 5′-GG-3′ sequences in double-stranded DNA by UV radiation with riboflavin, J. Biol. Chem. 268 (1993) 13221–13227.
[29] H. Mizutani, Y. Hiraku, S. Tada-Oikawa, M. Murata, K. Ikemura, T. Iwamoto, Y. Kagawa, M. Okuda, S. Kawanishi, Romidepsin (FK228), a potent histone deacetylase inhibitor, induces apoptosis through the generation of hydrogen peroxide, Cancer Sci. 101 (2010) 2214–2219.
[30] J.B. Sampson, J.S. Beckman, Hydrogen peroxide damages the zinc-binding site of zinc-deficient Cu, Zn superoxide dismutase, Arch. Biochem. Biophys. 392 (2001) 8–13.
[31] S. Ohnishi, S. Kawanishi, Double base lesions of DNA by a metabolite of carcinogenic benzo[a]pyrene, Biochem. Biophys. Res. Commun. 290 (2002) 778–782.
[32] S. Kawanishi, S. Inoue, S. Sano, Mechanism of DNA cleavage induced by sodium chromate(VI) in the presence of hydrogen peroxide, J. Biol. Chem. 261 (1986) 5952–5958.
[33] D.W. Celander, T.R. Cech, Iron(II)-ethylenediaminetetraacetic acid catalyzed cleavage of RNA and DNA oligonucleotides: similar reactivity toward single- and double-stranded forms, Biochemistry 29 (1990) 1355–1361.
[34] D.M. Leach, N.J. Zacal, A.J. Rainbow, Host cell reactivation of gene expression for an adenovirus-encoded reporter gene reflects the repair of UVC-induced cyclobutane pyrimidine dimers and methylene blue plus visible light-induced 8-oxoguanine, Mutagenesis 28 (2013) 507–513.
[35] Y. Hiraku, K. Ito, K. Hirakawa, S. Kawanishi, Photosensitized DNA damage and its protection via a novel mechanism, Photochem. Photobiol. 83 (2007) 205–212.
[36] S. Oikawa, S. Kawanishi, Site-specific DNA damage induced by NADH in the presence of copper(II): role of active oxygen species, Biochemistry 35 (1996) 4584–4590.
[37] M.J. Burkitt, Copper–DNA adducts, Methods Enzymol. 234 (1994) 66–79.
[38] S.M. Chiu, L.Y. Xue, L.R. Friedman, N.L. Oleinick, Differential dependence on chromatin structure for copper and iron ion induction of DNA double-strand breaks, Biochemistry 34 (1995) 2653–2661.
[39] Y. Li, M.A. Trush, Reactive oxygen-dependent DNA damage resulting from the oxidation of phenolic compounds by a copper-redox cycle mechanism, Cancer Res. 54 (1994) 1895s–1898s.
[40] R.G. Stevens, D.Y. Jones, M.S. Micozzi, P.R. Taylor, Body iron stores and the risk of cancer, N. Engl. J. Med. 319 (1988) 1047–1052.
[41] T. Tanaka, Y. Iwasa, S. Kondo, H. Hiai, S. Toyokuni, High incidence of allelic loss on chromosome 5 and inactivation of p15INK4B and p16INK4A tumor suppressor genes in oxystress-induced renal cell carcinoma of rats, Oncogene 18 (1999) 3793–3797.
[42] E. Kukielka, A.I. Cederbaum, Ferritin stimulation of hydroxyl radical production by rat liver nuclei, Arch. Biochem. Biophys. 308 (1994) 70–77.
[43] W.J. Malaisse, J.C. Hutton, S. Kawazu, A. Herchuelz, I. Valverde, A. Sener, The stimulus-secretion coupling of glucose-induced insulin release. XXXV. The links between metabolic and cationic events, Diabetologia 16 (1979) 331–341.
[44] R.G. Sturmey, C.P. Wild, L.J. Hardie, Removal of red light minimizes methylene blue-stimulated DNA damage in oesophageal cells: implications for chromoendoscopy, Mutagenesis 24 (2009) 253–258.